TECHNICAL PAPER

ISSN 1047-3289 *J. Air & Waste Manage. Assoc.* **53**:347–359


# Urban Photochemical Pollution in the Iberian Peninsula: Lisbon and Barcelona Airsheds

**Nelson Barros**
*Department of Science and Technology, University of Fernando Pessoa, Porto, Portugal*

**Carlos Borrego**
*Department of Environment and Planning, University of Aveiro, Aveiro, Portugal*

**Isabel Toll, Cecilia Soriano, Pedro Jiménez, and José Maria Baldasano**
*Laboratory of Environmental Modeling, Technical University of Catalonia, Barcelona, Spain*

## ABSTRACT
Numerical simulations with photochemical transport models were independently performed for two domains situated in the Iberian Peninsula covering the Lisbon and Barcelona airsheds. Although the days chosen for simulation of the two cities are not the same, the synoptic situations in both cases, known as typical summertime situations, were similar, which allowed the development of typical mesoscale circulations, such as sea breezes and mountain and valley winds dominated by the Azores anticyclone. Emission inventories for the two areas were developed. The $O_3$ concentrations recorded in both cities have a similar level. Nevertheless, $O_x$ values in Barcelona are higher than in Lisbon, which may, at a first glance, indicate an apparently more oxidant atmosphere in Barcelona. Photochemical modeling for the two cities has shown that the behavior of the circulatory patterns in both urban areas is rather different, which mainly has to do with the different strengths of the sea breeze and the topography, inducing an important offshore vertical layered dimension of pollutant transport in Barcelona versus an important inland horizontal transport in Lisbon.

**IMPLICATIONS**

The study of the generation and transport of tropospheric $O_3$ in southern Europe is a subject of special interest. This paper compares the diverse circulation patterns between the most important coastal cities in the Iberian Peninsula, Lisbon and Barcelona, by using the grid-based photochemical transport models MAR IV (Modelo Atmosférico Regional) and Model for the Atmospheric Dispersion of Reactive Species, respectively. Results suggest that factors controlling transport and diffusion in these two coastal regions are largely on the local scale, and dispersion conditions are highly complex and site-specific. Mesoscale transport phenomena play an important role. Ozone levels can be very dissimilar for both cities, because different topographic conditions may lead to different $O_3$ transport and concentrations under the same meteorological situation.

## INTRODUCTION
During the last few years, great importance has been placed on the study of regional-scale forcing on the formation of specific air quality conditions, especially on the coastal areas, and it has been widely reported that significant degradation of air quality in some areas can be attributed to mesoscale transport phenomena.[1–5] Numerical simulations of photochemical transport were performed for the regions of Lisbon and Barcelona to study the similarities and differences of the photochemical transport patterns in two regions subject to high anthropogenic stress during a typical summertime situation from the synoptic point of view, usually dominated by the Azores anticyclone. Under such synoptic situations, characterized by a very weak large-scale forcing, Lisbon and Barcelona, being located respectively at the western and eastern coastal edges of the Iberian Peninsula, can attain high values of $O_3$ concentration, often exceeding European Union standards for that pollutant.

The two regions under consideration are located in the Iberian Peninsula next to large water bodies (the Atlantic Ocean and the Mediterranean Sea, for Lisbon and Barcelona, respectively) and have a complex topography, leading to the development of mesoscale phenomena, such as sea breezes and slope and valley winds. However, local specific characteristics lead to a different development or intensity of these mesoscale phenomena in the case of weak synoptic meteorological conditions. For instance, the different topographies of both urban areas and the cooler waters of the Atlantic Ocean, as opposed to the warmer Mediterranean Sea, lead to a different development of the sea breeze during the day. The important vertical dimension of the circulatory patterns of air masses in the region was also studied for Barcelona, resulting in a multilayer arrangement of pollutants.[6,7] On the other hand, in the Lisbon region, the mesoscale circulation is, in general, reinforced by the north-northwest synoptic circulation associated with the Azores anticyclone promoting a strong circulation from the sea, which induces a relatively less expressive dimension to the vertical circulations.[8,9] The comparison of the two scenarios has shown how different transport behavior can be in two locations that share similar synoptic conditions and complex orography and land/sea interfaces, thus demonstrating that air pollution management and reduction policies are not universal and that specific plans must be carried out for every location where pollution reduction measures are being adopted.

## DESCRIPTION OF THE LISBON AND BARCELONA AIRSHEDS

### Geomorphologic Description

The two airsheds considered in this study are (1) a 106 × 86 km$^2$ area centered on the city of Lisbon, located on the western coast of the Iberian Peninsula close to the Atlantic Ocean; and (2) an area of 80 × 80 km$^2$ centered on the city of Barcelona, located on the northeastern coast and close to the Mediterranean Sea. Both domains and their main orographic characteristics are represented at the bottom of Figure 1. Another important fact is that the domain under consideration in Lisbon has a population of approximately 3.5 million inhabitants, while the domain considered for the Barcelona area includes more than 4.3 million inhabitants.

Lisbon is built near the Tagus estuary (320 km$^2$) in a zone with a complex coastline associated with a gently rolling terrain and multiple hills reaching more than 400 m above sea level (ASL) (Montejunto, 666 m; and Sintra, 528 m). To the south, the coastline is still sinuous and complex, and the domain is dominated by the Sado estuary (more than 135 km$^2$) and Arrábida hill (501 m). To the interior, the Tagus and Sado river valleys are the major orographical features.

The topography of Barcelona is more complex than that of Lisbon. It has two mountain ranges parallel to the coast. Between the coastline and the coastal range, there is the coastal depression, where the city of Barcelona is located. The main peaks of the coastal range have altitudes between 500 and 650 m ASL. On the other hand, the precoastal range, further from the coastline, has higher altitudes, between 1100 and 1200 m ASL in the domain of study. The precoastal depression is located between the coastal and the precoastal ranges. Another important feature of this area is that the coastal depression is linked to the prelittoral range through the valleys of Llobregat and Besos, which are perpendicular to the coastline.

Figure 2 shows the percentage distribution of the main land use of the simulation domains in both geographical areas. As can be clearly observed, Barcelona presents equilibrium between the percentage of forests, agriculture, and other land use, which in this case are mainly shrub lands, while urban areas (category that also includes communication network and industrial areas) make up 15% of total land use. In contrast, Lisbon contains a relatively larger extension of forest and agriculture area and less than half of the urban Barcelona area. Table 1 is a summary of the main aspects of both metropolitan areas and shows their similarities and their differences.

### Meteorology

Particular orographic characteristics lead to different local wind patterns in both regions, even under similar synoptic-scale conditions. To show these differences, daily evolutions of wind speed and direction are represented in Figure 3 for two stations in Barcelona (Montcada and Airport) and for two stations in Lisbon (Cabo da Malha and Airport). Data shown are from the days simulated for this work, which, as will be shown later, can both be described as typical summertime days from the synoptic point of view, with conditions that lead to the development of mesoscale circulations in the region.

In the summertime, depending on the Azores anticyclone relative position and intensity in the North Atlantic and the position of its extension over the northern part of the Iberian Peninsula, Portugal can be under a synoptic forcing essentially from the north or east-northeast. The Portuguese coast essentially has a north-south orientation, which means that the sea breeze is strongly dependent on the direction and strength of that synoptic forcing. When synoptic forcing is from the north, the sea breeze has an early start and a strong presence. In the case of an east-northeast synoptic forcing, the sea-breeze mesoscale circulation, essentially from the west-northwest, is delayed and attenuated by the east-northeast synoptic forcing. In the study case in Lisbon, forcing was from the east-northeast, which promoted a relatively strong circulation from the north-northeast during the night and morning over the Lisbon region. In this case, the sea-breeze mesoscale circulation from the west, in particular in the Cabo da Malha coastal station (50 km south of Lisbon), is retarded and attenuated by the north-northeast flow. Nevertheless, the presence of the sea-breeze circulation is recognized by an abrupt shift of the wind direction at 1000 Coordinated Universal Time (UTC) at the Cabo da Malha station and around noon at Lisbon Airport. The distance to the coastline from Lisbon Airport

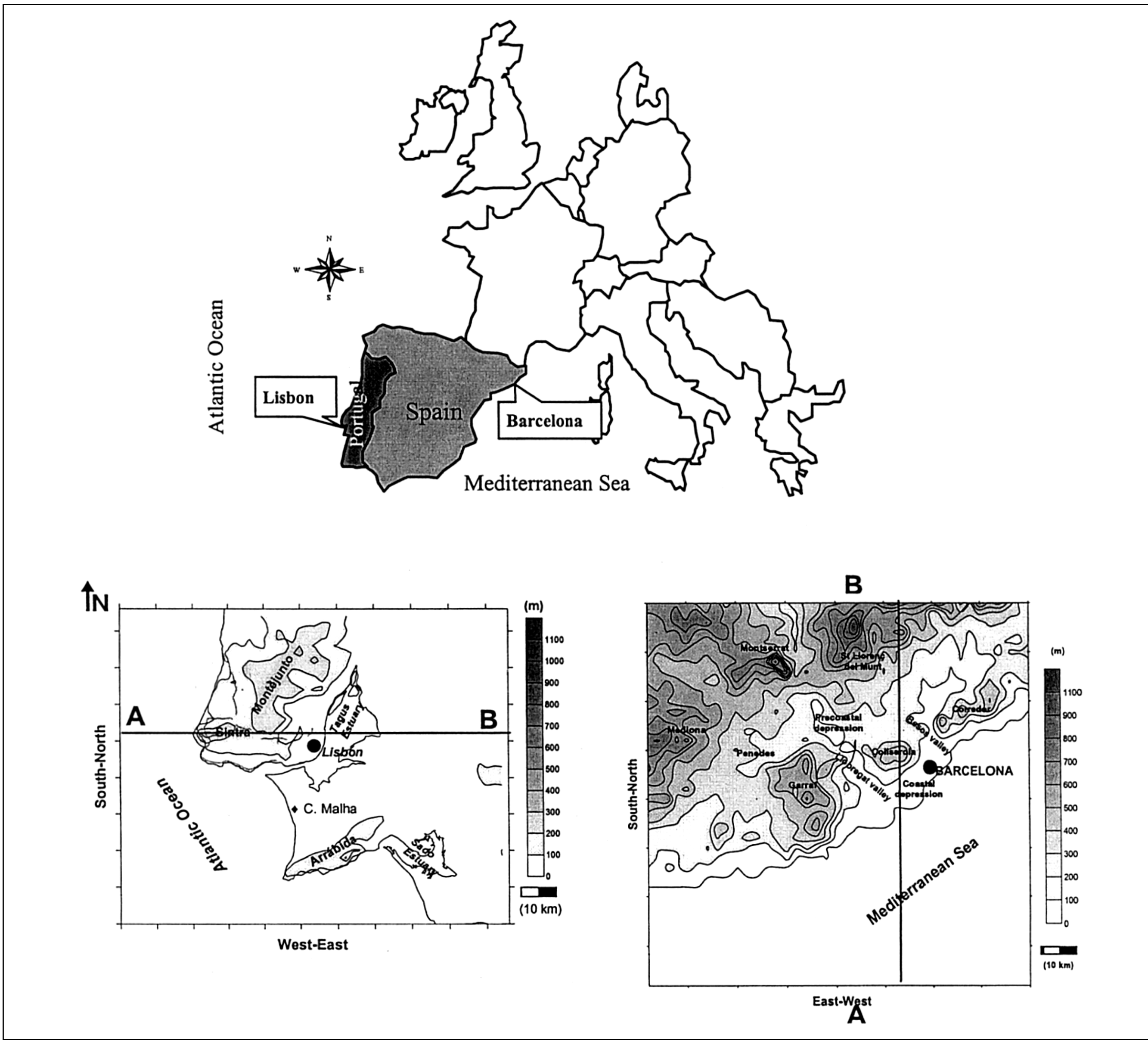


**Figure 1.** Lisbon and Barcelona localizations on the Iberian Peninsula (top), simulation domains for Lisbon (bottom left) and Barcelona (bottom right), and their main orographic features (A-B cross section line, see Figures 8 and 9).

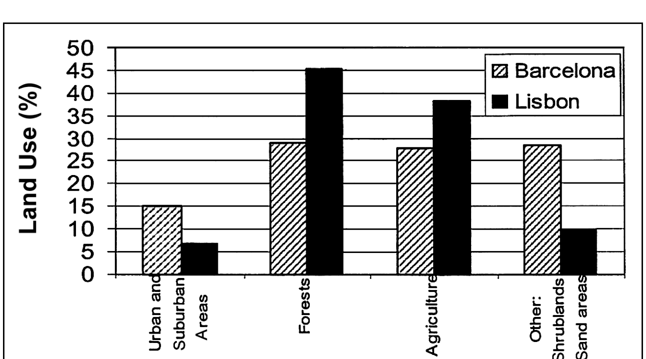


**Figure 2.** Percent distribution of the main land uses in both domains.

**Table 1.** Main aspects concerning Lisbon and Barcelona metropolitan areas.

| Lisbon Area | Barcelona Area |
|---|---|
| • Summer meteorological situation that permits the development of mesoscalar flows: land-sea breeze and anabatic-katabatic circulations<br>• Location at Atlantic coastal zone in the Iberian Peninsula<br>• Rolling terrain: Tagus and Sado estuaries and mountain (less than 700 m ASL) near the coast<br>• Complex coastal line | • Summer meteorological situation that permits the development of mesoscalar flows: land-sea breeze and anabatic-katabatic circulations<br>• Location at Mediterranean coastal zone in the Iberian Peninsula<br>• Complex terrain: several valleys perpendicular to the coastal line, two mountain ranges: coastal (500 m ASL) and precoastal (1000–1200 m ASL)<br>• Linear coastal line |

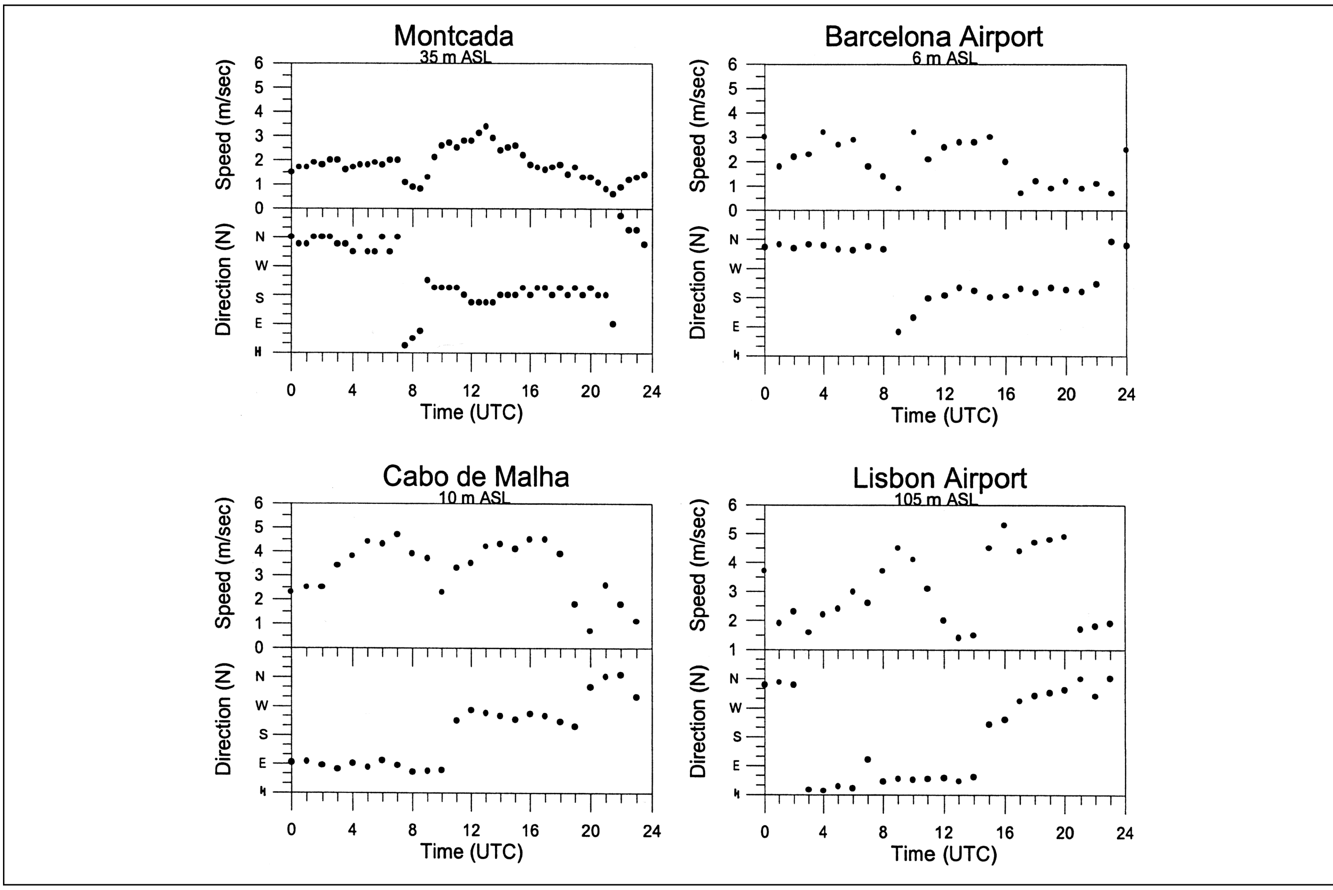


**Figure 3.** Daily evolution of wind speed and direction for stations in Barcelona (top) (August 5, 1990) and Lisbon (bottom) (July 10, 1996).

(20 km from the Atlantic coast) can explain the sea-breeze delay.

In the stations of the Barcelona region, the daily evolution of wind speed and direction very clearly shows the influence of the sea breeze in these variables. The pass from the nighttime to the daytime regime is evident in the graph and can be identified both by a sudden change in wind direction and by very low wind speeds during the transition period. Both stations show that this transition takes place around 900 UTC. Sunrise at this time of the year takes place, approximately, at 600 UTC, and the system needs a few hours of insolation for the sea breeze to develop. Note that the start of the sea-to-land breeze takes place a little earlier in the Airport station than in the Montcada station. This has to do with the seaside location of the former location, while the latter is located a few kilometers inland and, therefore, the sea breeze needs some time to penetrate there. The on-shore regime spans for more than 8 hr in Barcelona.

## Air Quality

Air quality in both areas is compared by means of data on concentrations of air pollutants collected between 1989 and 2000 in some surface measurement stations. Only one measurement station is considered in the Lisbon domain (Século), while data from five surface measurement stations (Montcada, Hospitalet, Molina, Poble Nou, and Badalona), all of which can be considered urban stations, were available in the area of Barcelona for the same time period. Because the present work focuses on analysis of $O_3$ levels, annual mean $O_3$ concentration, the mean annual daily maximum of $O_3$ concentration, and the annual mean $O_x$ ($O_3 + NO_2$) concentration have been plotted for analysis in Figure 4.

The $O_3$ annual mean and the annual mean of the daily maximum concentration values registered in the Século station were similar to those registered in the Barcelona area. For 1989–1993, the $O_3$ annual mean had values between 30 and 40 $\mu g/m^3$ and increased to 35–45 $\mu g/m^3$ in the period 1994–2000. These annual $O_3$ values are slightly lower than the European annual $O_3$ limit of 40–60 $\mu g/m^3$ as an average.[10] Finally, the annual mean maximum concentration values vary between 70 and 80 $\mu g/m^3$ at the beginning of the period considered and later increase to 90–100 $\mu g/m^3$.

The highest mean $O_x$ concentrations in the Molina station are typical of an urban location close to road traffic emissions, as is the case. In general, higher values of mean $O_x$ concentrations were registered in the urban measurement stations of the Barcelona area than in that

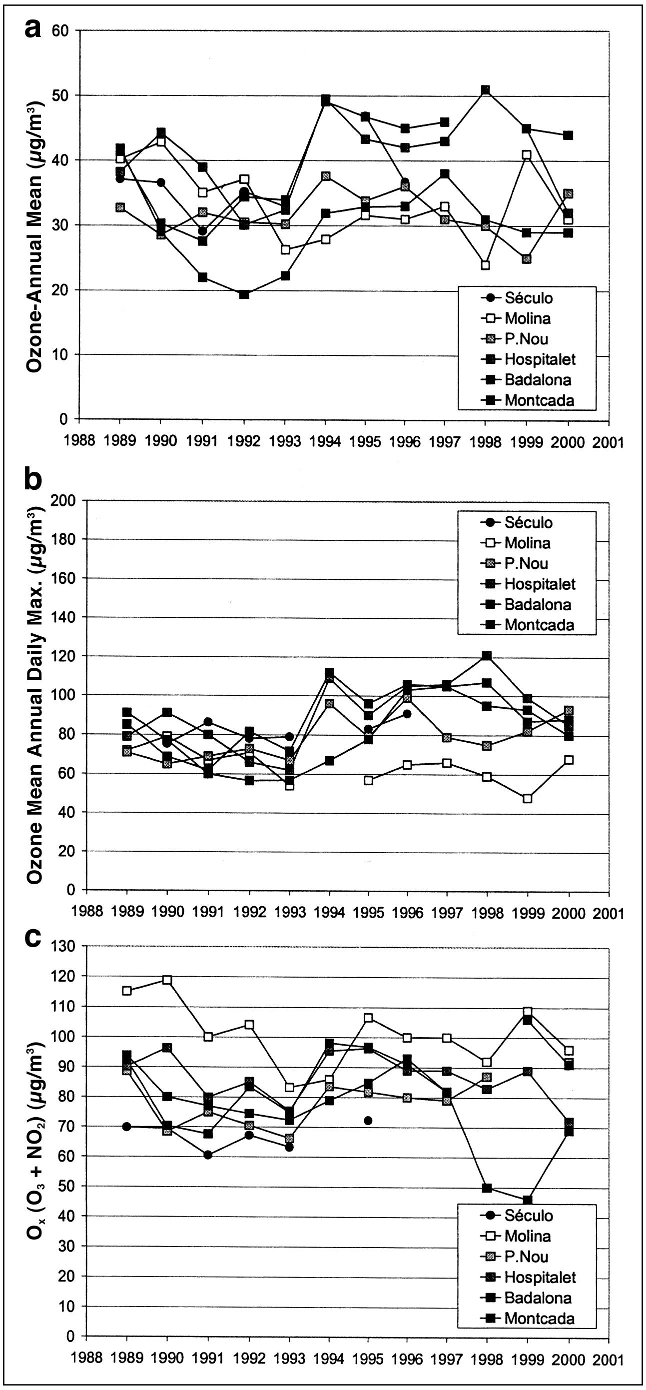


**Figure 4.** (a) $O_3$ annual mean; (b) annual mean of the daily $O_3$ maximum; and (c) $O_x$ ($O_3$ + $NO_2$) annual mean for Lisbon (circles) and Barcelona (squares). All units are $\mu$g/m$^3$.

of Século. At first glance, this could indicate a more oxidant atmosphere in Barcelona, which implies much higher $NO_2$ levels. It is also interesting to study the daily evolution of $O_3$ concentrations in both locations. Figure 5 shows $O_3$, $NO_2$, and NO concentrations as a function of time of day for two stations in the Lisbon area and two stations in Barcelona for their respective simulated days.

Data from the Molina and Hospitalet stations in Barcelona area show that $O_3$ levels are low during the nighttime and begin to rise as soon as the sun rises and photochemical activity starts. Reduction of $O_3$ levels during the first hours of the morning, with low solar activity, is associated with increasing emissions of NO during rush hour, which depletes $O_3$. Solar irradiation later on and emission of precursors ignite production of $O_3$, which is built up rapidly (because the mixing layer is still shallow) and peaks after solar midday, between 1200 and 1400 UTC. After sunset, the depletion of $O_3$ starts, but its consumption is slower than its formation during the early morning.

In Lisbon, unfortunately, for the Século station, only $O_3$ data was recorded, and NO and $NO_2$ data are not available. However, data from the Entrecampos street station (Lisbon center) were available and are included and discussed to complete the lack of information. As shown, in general, the $O_3$ level in both Lisbon stations is relatively low, reflecting the urban characteristics of these stations. Note that Século and Entrecampos $O_3$ concentration levels show a difference, which can be easily explained by taking into account their relative distance from the street emissions. The Entrecampos station is on the side of a very high-traffic avenue and the Século station is placed at a third-stage roof in a relatively quiet road.

## CASE STUDY

### Summer Meteorological Situation: Description of the Meteorological Approach

The most frequent summer synoptic meteorological situation over the Iberian Peninsula is characterized by a slightly high sea-level pressure and almost nonexistent surface pressure gradients over the domain.[11] This weak pressure gradient is called barometric swamp and is formed on approximately 70% of the summer days. It is associated with weak winds in the lower troposphere, cloudless skies, high maximum temperatures, and weak precipitation rates. Under this weak synoptic forcing, strong insolation promotes the development of prevailing mesoscale flows associated with the local orography (anabatic and katabatic winds), while the temperature difference between the sea and the land enhances the development of sea-land breezes.

In Barcelona, the mean air temperature during summer is 23 °C and the mean maximum air temperature is approximately 27 °C,[12] while the water temperature of the Mediterranean Sea in the region during this time of the year is 24 °C. On the other hand, in Lisbon, the mean maximum air temperature during summer is approximately 30 °C, while the mean water temperature of the

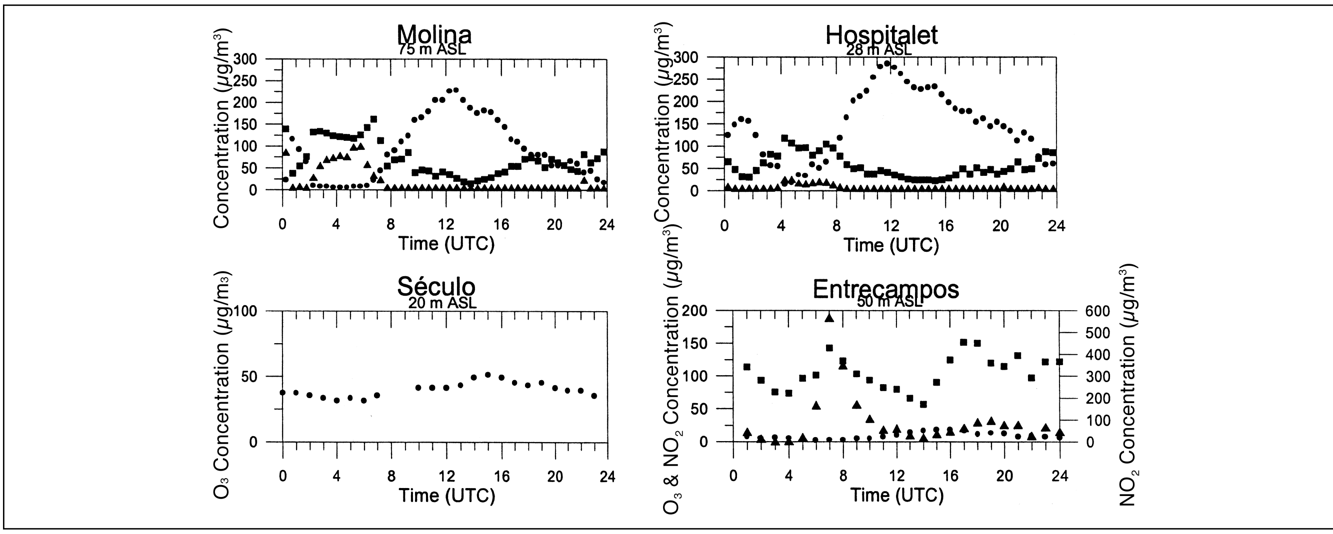


**Figure 5.** Daily evolution of concentration of $O_3$ (circles), $NO_2$ (squares), and NO (triangles) for stations in Barcelona (top) (August 5, 1990) and Lisbon (bottom) (July 10, 1996).

Atlantic Ocean in summer is around 16 °C. Therefore, while in the Barcelona area, the maximum gradient of temperatures between the sea and the land can be around 10 °C, in the Lisbon area, it can reach more than 20 °C.[13] This leads to a significant difference between both areas, especially regarding the sea-land breeze developing potential.

The Lisbon simulation was performed for day 3 (July 10, 1996) of the experimental campaign LisbEx 96.[13] This day is an example of the most frequent synoptic meteorological situation during summer, normally dominated by an extension of the Azores anticyclone over the northern part of the Iberian Peninsula. Strong insolation promotes the formation of mesoscale circulations and photochemical production. The Barcelona simulation was performed for August 5, 1990, a day with low geostrophic forcing and high insolation. In fact, a photochemical pollution episode took place between August 3 and 5, 1990, and during the same period, high $O_3$ concentrations were registered in central and northern Europe.[14,15]

Figure 6 shows the synoptic surface charts for the two simulated days. The synoptic chart for the Lisbon simulation day shows separated isobars over the study region, which is indicative of a relatively weak synoptic forcing. Data from the radiosonde acquired that day showed a north-northeast forcing over Lisbon. The map corresponding to the simulation of Barcelona also showed much-separated isobars, indicating a low synoptic forcing over the modeled region. A weak northeastern forcing was observed in the radiosondings launched in either Lisbon or Barcelona and can also be inferred from the 1020 hPa isobar crossing the Peninsula.

## Development and Results of the Emission Inventories

Emission inventories had to be developed for both areas to get the emission data, which, together with the results from the meteorological model, were used as input for the application of the photochemical transport model. To estimate hourly emissions in the Lisbon area, the so-called top-down approach was used for most of the sources.[16] A bottom-up approach was used for the estimation of emissions in the Barcelona area.[17]

Traffic emissions in both domains were calculated essentially following the Core Inventory of Air Emissions (CORINAIR) emission factors and methodology. Nevertheless, in Lisbon, the bottom-up methodology was only applied to main roads, such as highways and interregional roads. All other emissions from local roads and from urban traffic were considered area sources. The methodology employed for the biogenic emissions was the same in both domains and is based on previous works[18,19] that take into account local vegetation data (land-use distribution and biomass factors) and meteorological conditions (surface air temperature and solar radiation). The main difference in both methodologies is that in the Lisbon domain, the emissions coming from agricultural plant species were not considered, but agriculture emissions related to the use of fertilizers, which have been included in the category of "other anthropogenic sources," were considered. In this category, different anthropogenic sources were considered, as shown in Table 2. In the Lisbon domain, only the greatest industries were considered point sources with available measured data. The other industrial emissions were considered surface emissions spatially disaggregated from the CORINAIR 90 inventory.[16]

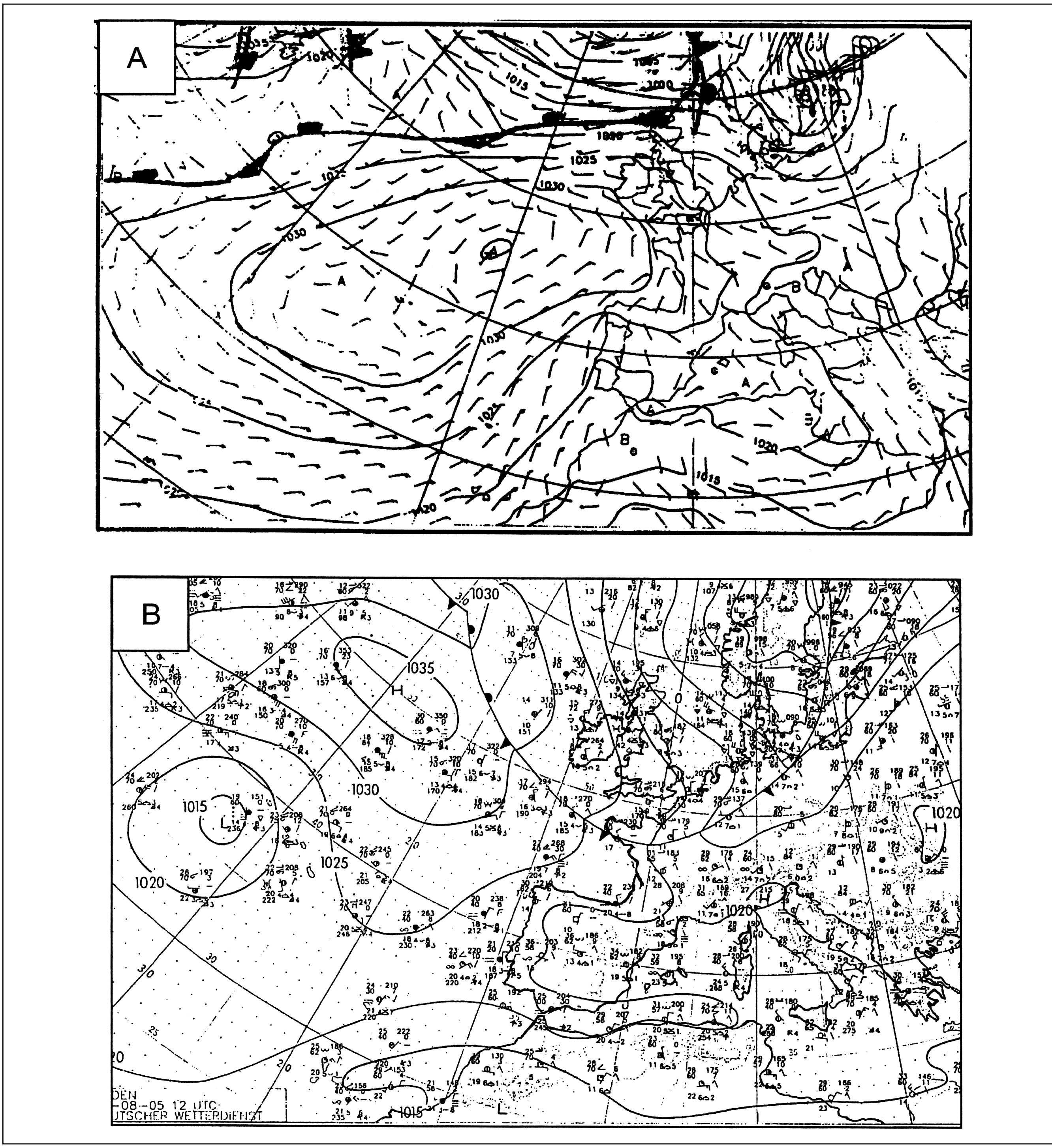


**Figure 6.** (a) Lisbon surface synoptic chart for July 10, 1996, at 1200 UTC; and (b) Barcelona surface synoptic chart for August 5, 1990, at 1200 UTC.

In the comparison of both inventories, it must be taken into account that the domain considered for Lisbon is approximately 30% larger than the domain considered for Barcelona. However, the population living in Barcelona's domain is approximately 20% higher than the population in Lisbon. Keeping in mind these constrains, the emission amounts in both areas were compared and analyzed (Table 3).

For all pollutants, the total emissions estimated for the Lisbon area were higher than the total emissions estimated for the Barcelona area. This apparent inconsistency may be explained by three main factors: (1) biogenic emissions are much higher in the Lisbon area, because of a larger area of forest and agriculture in the Lisbon domain; (2) the Lisbon area has heavier industry than Barcelona, such as power plants and pulp and paper

**Table 2.** Sources included in the category "other anthropogenic sources" for both geographical areas of Lisbon and Barcelona.

| Lisbon Area | Barcelona Area |
|---|---|
| Industrial activities (as point sources) | Industrial point sources |
| Industrial activities (as area sources) | Petrol stations |
| Extraction and distribution of fuels | Port tanks |
| Solvent use | Residential and commercial activities |
| Agriculture (fertilizers) | Maritime traffic |
| Residential and commercial activities | Airport traffic |

factories; (3) Barcelona has a networked distribution of natural gas for industrial and domestic uses, as opposed to Lisbon, where, at the time of the present emission inventory, domestic gas distribution was only available in the urban area of Lisbon (currently, almost all the Lisbon area has natural gas distribution). The differences found in road traffic emissions can be explained by the larger domain defined in Lisbon or by different methodologies and associated estimation errors.

To account for these differences, a comparison of emissions per km$^2$ and per capita also was performed and gave highest values for the Lisbon area in general. In the Barcelona area, road traffic is clearly the main emission source with a strong difference from the other sources. The contribution of biogenic activity to VOC emissions is also significant. Of the pollutants emitted, CO is the highest followed by VOC, $NO_x$, and $SO_2$. In the Lisbon area, road traffic is the main emission source of CO and contributes significantly to VOC and $NO_x$ emissions. The greatest contribution to VOC emissions comes from biogenic activity. The "other anthropogenic sources" contribute significantly to $NO_x$ and $SO_2$ emissions. In relation with the pollutants emitted, as in Barcelona, CO is the highest, followed by VOC, $NO_x$, and $SO_2$.

Estimation shows that Barcelona has a VOC/$NO_x$ ratio of 1.56 and Lisbon has a ratio of 1.08, which reflects the strong role played by $NO_x$ emissions emitted under the category "other anthropogenic sources" in Lisbon compared with Barcelona. Apparently, the whole Lisbon area has a higher oxidant atmosphere than the whole Barcelona domain when using estimates from the emission inventories for comparison. However, the relative importance of the road traffic in Barcelona, with a much larger urban area, can explain the greater levels of $O_x$ found there when comparing emission measurements.

## Description of the Models Used and the Model Setup

*Lisbon Simulations*. To consider mesoscale atmospheric circulations in the study of atmospheric dispersion patterns and, in particular, the analysis of photochemical pollution in the region of Lisbon, a version of Systems Applications International Mesoscale Model (SAIMM),[20] a prognostic 3-day meteorological model, was used to generate the meteorological inputs needed by the Urban Airshed Model (UAM-CB IV). The winds were vertically averaged within the UAM layers at each horizontal grid location and hour to generate the UAM wind fields, taking into account the mixing height predicted by the SAIMM. The UAM surface-temperature field was generated by converting the SAIMM surface potential temperatures to actual temperatures. This integrated system, which was especially developed to be applied to coastal regions, was named MAR IV (Modelo Atmosférico Regional).[9] The MAR IV system has been evaluated with experimental data, and its performance has been compared with that of other models.[9,21] In both cases, the system is consistent and gives realistic results.

The application of the MAR IV system to day 3 (July 10, 1996) of the experimental campaign LisbEx 96 was performed over a modeling domain of 106 $\times$ 86 km$^2$ centered in the city of Lisbon with a horizontal grid spacing of 2 $\times$ 2 km$^2$. In the vertical direction, the grid consists of 28 non-equidistant layers up to 8000 m for the

**Table 3.** Daily emissions (kg/day) on a summer day for the Lisbon Area (summer day in 1992) and the geographical area of Barcelona (weekend summer day in 1990).

| | VOCs | | $NO_x$ | | CO | | $SO_2$ | |
|---|---|---|---|---|---|---|---|---|
| | Lisbon | Barcelona | Lisbon | Barcelona | Lisbon | Barcelona | Lisbon | Barcelona |
| Road traffic (t/yr) | 87,587 | 67,259 | 12,723 | 74,401 | 619,327 | 428,013 | 8449 | 9260 |
| | (31%) | (51%) | (48%) | (89%) | (71%) | (98%) | (13%) | (81%) |
| Biogenic (t/yr) | 147,278 | 44,171 | | | | | | |
| | (51%) | (34%) | | | | | | |
| Other anthropogenic sources (t/yr) | 51,853 | 19,363 | 137,854 | 9588 | 250,053 | 7657 | 60,954 | 2170 |
| | (18%) | (15%) | (52%) | (11%) | (29%) | (2%) | (87%) | (19%) |
| Total (kg/day) | 286,713 | 130,793 | 265,084 | 83,989 | 869,380 | 435,670 | 70,004 | 11,430 |
| Total (kg/day/km) | 31.45 | 20.45 | 29.08 | 13.12 | 95.37 | 68.07 | 7.68 | 1.79 |
| Total (kg/day/inhab) | 0.082 | 0.031 | 0.076 | 0.019 | 0.248 | 0.102 | 0.017 | 0.003 |

mesometeorological model and seven layers up to 3 km for the photochemical dispersion model, four below the mixing layer and three above. The synoptic forcing to initialize the mesoscale model was derived from data of a radiosonde launch in Lisbon airport. The model sea-surface temperature was considered to be domain-constant and equal to the average of online sea-surface temperature read at an open-sea sonde located northwest of Lisbon. A previous-day dispersion simulation with the same meteorological and emission data was used as the initial conditions for the pollutant concentrations in the photochemical dispersion run.

*Barcelona Simulations.* The simulations in Barcelona were carried out with the meteorological nonhydrostatic Mesoscale Model and the three-dimensional Model for the Atmospheric Dispersion of Reactive Species.[22] This was applied with the chemical mechanism from the European Monitoring and Evaluation Program (EMEP),[23] which describes the tropospheric gas-phase chemistry with 66 species and 139 photochemical reactions. VOC emissions were split into the 13 categories considered in the EMEP mechanism for each emitting source depending on its characteristics. The meteorological and photochemical dispersion simulations were conducted in the same domain of 80 $\times$ 80 km$^2$ with a horizontal resolution of 2 $\times$ 2 km$^2$. The upper boundary was set to a height of 6000 m ASL and the airshed was divided vertically into 35 levels for the meteorological run, while the photochemical dispersion run was performed in the first 30 layers of those used for the meteorological run.[24]

The simulation was performed for August 5, 1990, the last day of the photochemical pollution episode that took place between August 3 and 5, 1990. The analysis of $O_3$ concentration data from five surface measurement stations in the area of Barcelona showed that maximum values were reached within the urban area core: Plaça Molina (228 $\mu$g/m$^3$) and Hospitalet de Llobregat (284 $\mu$g/m$^3$). A previous-day dispersion simulation with the same meteorological and emission data was used as the initial condition for the pollutant concentrations in the photochemical dispersion run. Inflow lateral boundary concentrations were derived by spatially interpolating the results from a simulation with the Lagrangian EMEP MSC-W model for Europe, which gave as input an $O_3$ concentration range between 28 and 126 $\mu$g/m$^3$.

## DESCRIPTION OF THE SUMMER MESOSCALE AIRFLOW PATTERNS IN THE LISBON AND BARCELONA AREAS

The complex wind circulation and, in particular, the $O_3$ formation and transport in the Lisbon and Barcelona domains were visualized by the application of mesoscale modeling tools (Figure 7) and analyzed in this section. At 500 UTC (see Figures 7a and 7e), a land breeze is established in both domains. However, the land breeze is stronger in the Barcelona area, because of the development of katabatic winds on the southern slopes of the main mountain ranges, which contribute to the reinforcement of the general offshore flow. In the Lisbon area, the mountains are lower than those in Barcelona. This would explain the weaker downslope flows established along its main mountain ridges. In both cases, channeling of the wind through the existing valleys is evident. In the Barcelona area, the valleys mainly channel the land breeze and katabatic winds toward the sea; in the Lisbon area, the Tagus valley channels the katabatic winds of the Montejunto mountain into the Tagus estuary, nearby Lisbon, and into the sea.

In Barcelona, during the early hours of the day and until 700 UTC, $O_3$ is depleted where NO is being emitted, mainly by road traffic both in the urban areas and at the main communication routes, producing as a result an increase in $NO_2$ concentration. At the same time, the land breeze, reinforced by katabatic and valley winds, transports this low $O_3$ concentration with $O_3$ precursors toward the Mediterranean Sea. In Lisbon, a similar process takes place at this time, with the precursors emitted in Lisbon during the morning rush hour being transported by the Tagus valley flow offshore toward the Tagus mouth.

The sea breeze begins to develop in the Barcelona area between 800 and 900 UTC. This transition situation between the nighttime and daytime regimes results in very low wind speeds in the whole domain. As the on-shore flow of the sea breeze is established in the following hours, it is reinforced in the Barcelona area, with the upslope winds developing on the southern slopes of the coastal mountain range developing the classic circulatory cell associated with the sea breeze. The photochemical formation of $O_3$ begins around 900 UTC in the planetary boundary layer (PBL). At the same time, the sea breeze causes the penetration of air masses loaded with $O_3$ and $O_3$ precursors from the Mediterranean Sea. The reinforcement of the sea breeze by the upslope winds in the coastal range, together with the increasing vertical mixing, drives ground air masses toward the upper layers of the PBL. This provokes a layer of high $O_3$ concentration at a height of around 600 m above the Llobregat valley.

In Barcelona, the sea breeze overcomes the coastal mountains after midday (see Figure 7b), transporting $NO_x$ emissions from road traffic inland, which, together with the higher biogenic VOC emissions in these hours, result in an $O_3$ concentration maximum in the precoastal depression. The sea-breeze front reaches the slopes of the precoastal mountain range, and important orographic injections taking place produce the uplift of $O_3$ and the

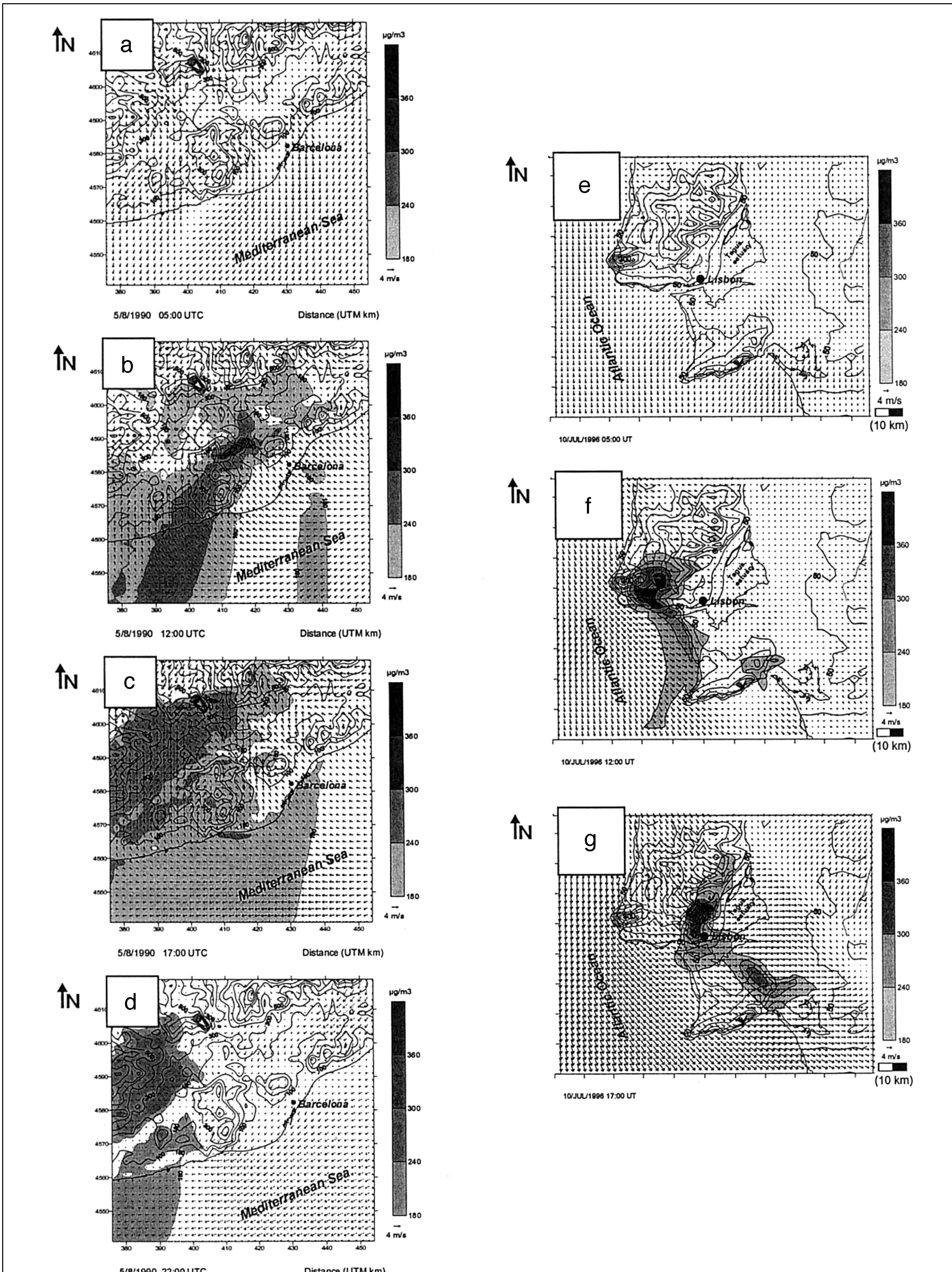
a
b
c
d
e
f
g
N
μg/m3
360
300
240
180
4 m/s
Barcelona
Mediterranean Sea
5/8/1990 05:00 UTC
5/8/1990 12:00 UTC
5/8/1990 17:00 UTC
5/8/1990 22:00 UTC
Distance (UTM km)
Lisbon
Atlantic Ocean
(10 km)
10/JUL/1996 05:00 UT
10/JUL/1996 12:00 UT
10/JUL/1996 17:00 UT

formation of elevated layers of pollutants between 1000 and 2000 m, observed during the evening.

The importance of the vertical circulations taking place in the region of Barcelona is evident in Figure 8, where a time series of a vertical south-to-north cross section of $O_3$ concentration fields simulated by the model in Barcelona at constant x-UTM = 420 km have been included. The plots show that, because of the sea-breeze front overwhelming the coastal mountain range and reaching the precoastal mountains, important orographic injections reach almost 2000 m ASL and produce the elevation to higher altitudes of $O_3$ and other pollutants emitted at the surface level.

The formation of elevated layers of pollutants in the region under typical summertime conditions has been studied in previous works and has been confirmed using lidar information acquired in the region during experimental campaigns.[6,7] These studies showed that the circulatory cell associated with the sea-breeze flow produces the penetration of pollutants inland, and its return flow causes the transport of pollutants aloft in an elevated layer disconnected from the surface. As the sea breeze penetrates further inland and its associated circulatory cell grows, its return flow takes place at higher altitudes and produces the positioning of air pollutants at higher levels. In Barcelona, this behavior is even more remarkable because the mountain ranges in the region, orientated parallel to the coastline, produce upslope winds that enhance this vertical transport and add new and higher elevated layers caused by topographic injections produced by the mountains.

In the subsequent hours and until 1700 UTC (as shown in Figure 7c), photochemical activity is lower but the previously formed $O_3$ is transported by the sea breeze and the anabatic winds toward the slopes of St. Llorenç del Munt and Montserrat. From 1800 UTC until the end of the day, the intensity of the solar radiation decreases sharply, provoking a depletion of the $O_3$ through reaction with NO in those places where this pollutant is emitted. Vertical mixing also decreases and decouples ground $O_3$ concentrations with those at higher air levels, which are advected toward the southwest by the geostrophic wind. The sea breeze becomes weaker at 1800 UTC, and the land breeze begins to flow at 2100 UTC.

During the early morning in the Lisbon area, the $O_3$ concentration is very low in the study domain, just above the background values. Ozone is depleted where NO is emitted, mainly by road traffic both in the urban areas and at the main communication routes. On the other hand, the precursors emitted in the Lisbon urban area during the morning rush hours are transported by the Tagus valley flow offshore toward the Tagus mouth. Over the ocean, the wind field is dominated by a northerly flow (500 UTC, Figure 7e).

At noon, a weak divergent flow is visible over the Tagus estuary and a sea-breeze front only a few kilometers inland. Slightly west of Lisbon, a stagnation zone is established near Sintra and the Tagus mouth. Part of the $O_3$ precursors emitted during the morning rush hour is retained in this stagnation area and another part is transported offshore. In Figure 9a, the local production of $O_3$ over Sintra hill can be observed. In the subsequent hours, the precursors and intensification of solar radiation allow the increase of the photochemical and mesoscale processes with a crucial impact on the local $O_3$ production and transport pattern. In Figure 9b, the vertical transport of $O_3$ plume over the Sintra hill because of a complex vertical circulation generated by the conjunction of the orographic injection promoted by the Sintra hill, the sea breeze penetration, and a prevalent weak estuary breeze can be observed. In Figure 7f, an $O_3$ surface plume advected by the sea breeze to the coast south of Lisbon is

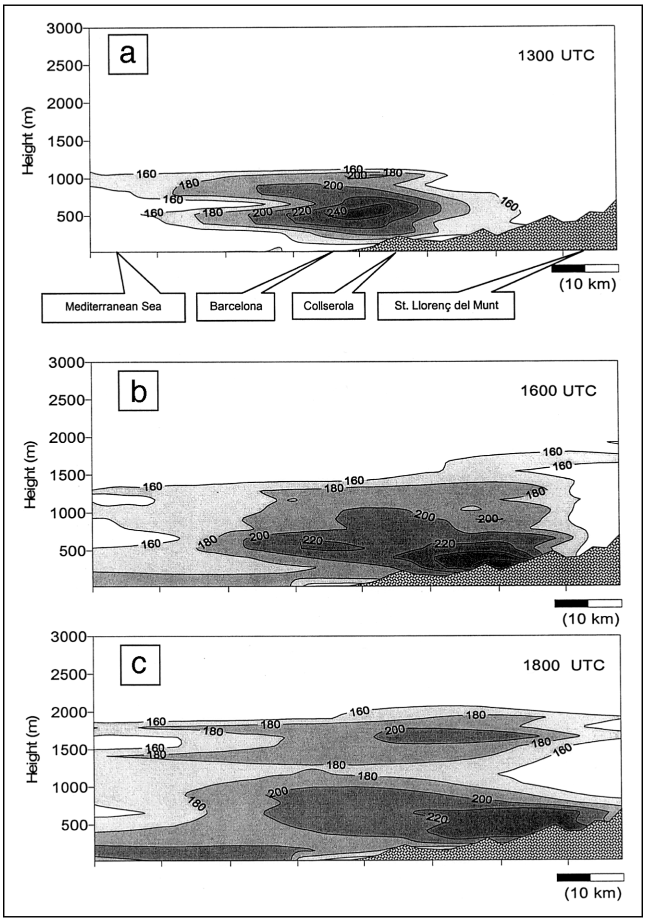


**Figure 8.** Time series of vertical south-north cross section of simulated $O_3$ concentration in $\mu g/m^3$ in Barcelona (see cross-section line in Figure 1).

**Figure 7.** Horizontal wind and $O_3$ concentration simulated for Barcelona at 500, 1200, 1700, and 2200 UTC (left) and Lisbon at 500, 1200, and 1700 UTC (right).

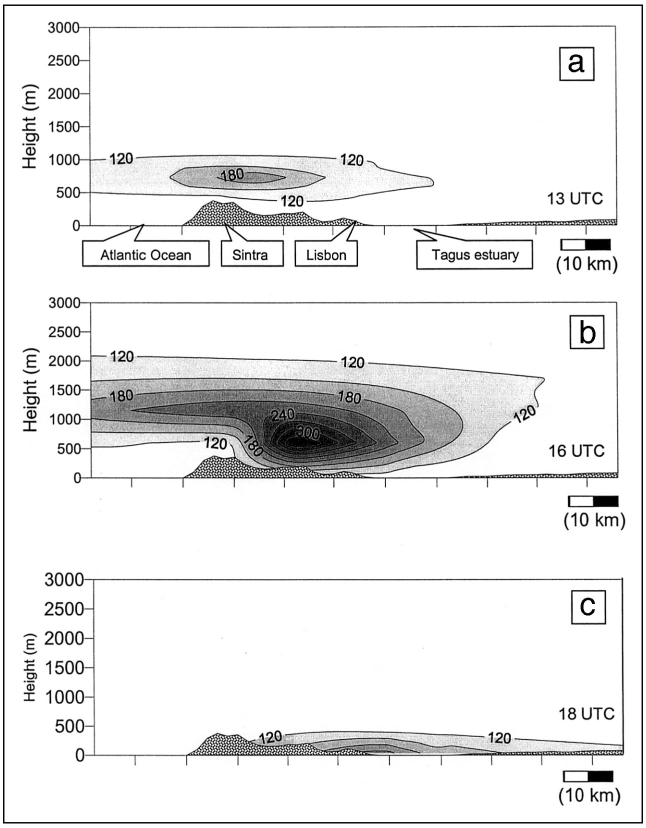


**Figure 9.** Time series of vertical west-east cross section of simulated $O_3$ concentration in $\mu g/m^3$ in Lisbon (see cross-section line in Figure 1).

visible, as is a relatively high $O_3$ concentration area over the stagnation area. At this time of the day, the precursor concentration decreases because of its participation in the photochemical process.

Late in the afternoon (1700 UTC, Figure 7g), a strong sea circulation along most of the coastline can be observed. This sea breeze, which is reinforced by the north-northwest synoptic circulation, is responsible for an important horizontal transport inland over the coastal zone of the relatively high $O_3$ concentration plume formed during the morning at the Sintra-Tagus mouth stagnation zone. This sea circulation also affects the vertical distribution of $O_3$, with an evident decrease of the observed levels and spreading (Figure 9c). After sunset, the photochemical processes stop and the $O_3$ concentration decreases, and onshore flow is gradually replaced by nocturnal drainage flow.

## CONCLUSIONS

The repercussion of meteorological conditions on air pollution by $O_3$ was studied in the two biggest Iberian Peninsula coastal cities: Lisbon and Barcelona. They present problems associated with tropospheric $O_3$ under the same summer meteorological context. The survey was made using numerical models for meteorology and photochemical dispersion, complemented by the corresponding emission inventories for both airsheds.

The synoptic situation studied is the typical behavior during the summer period (June, July, and August). This situation is a barometric swamp forced by the Azores anticyclone, which causes the emergence of mesoscale phenomena. It induces sea and land breezes and mountain winds, especially on the coasts.

The two zones present local aspects that differentiate them. Barcelona is located on the northwest coast of the Iberian Peninsula, presenting a complex topography with two rivers valleys that bring on canalizations perpendicular to the coast and two parallel coastal mountain ranges. On the other hand, Lisbon has a less elevated topography, dominated by the Tagus estuary and by an irregular coastline. Both urban centers favor an important formation of tropospheric $O_3$ caused by an equivalent synoptic situation that causes the atmospheric mesoscale circulation patterns derived from it to be dissimilar in horizontal and vertical transport.

In Barcelona, the sea-breeze circulation is reinforced and channeled by the main mountain upslope circulations and valley winds, respectively. The existence of a more complex topography in the Barcelona area, especially as far as the height of the surrounding mountains is concerned, leads to a very important vertical structure of the circulatory patterns, leading to the formation of pollutant layers disconnected from the surface, especially in the afternoon. In the sea-breeze process in Lisbon, the vertical dimension of the mesoscale phenomena is much more gentle and does not seem to play a very deterministic role in the dispersion of pollutants. The dominant circulation pattern in Lisbon exports $O_3$ with an inland horizontal transport in a southeast direction at sea level (<500 m) in the afternoon.

Results have shown that, under the same general conditions, topographic differences include that the development of mesoscale phenomena has patterns of $O_3$ advection and dispersion strongly linked to the mesoscale circulations. That influences tropospheric $O_3$ transport in the Lisbon and Barcelona areas. The results of the models show areas not covered by the air quality network, where the $O_3$ concentration might exceed the warning threshold as defined in the 2002/3/EC Directive.

These results highlight the different circulation patterns between Barcelona and Lisbon, induced by different topographic conditions under the same meteorological situation. Los Angeles has its own circulation pattern,[3,25] and this presents some similarities with the phenomenon that happens in Barcelona, taking into account the multiple factor scales (Pacific Ocean vs. Mediterranean Sea, topographic dimension, etc.). The factors controlling transport and diffusion in coastal regions are largely local-scale factors. Because these controlling factors are localized, dispersion conditions are highly complex and site-specific and are not often amenable to generalization.

## ACKNOWLEDGMENTS

This study was carried out under the framework of the European Union–funded project EUROTRAC, in the frame of subprojects SATURN and GENEMIS. The Catalan group also acknowledges support from the Generalitat de Catalunya, who funds the project IMMPACTE, and CICYT project REN2000–1020-C02–02. Simulations from the Barcelona group were performed on supercomputers belonging to CESCA (Centre de Supercomputació de Catalunya). The authors also would like to express their gratitude to PRAXIS XXI Program for their helpful support of AMAZOC (PRAXIS/3/3.2/AMB/38/94) and to the Portuguese General Directorate of Environment for their support of the Lisbon Photochemical Project (PEAM/P/AMA/603/95).

## REFERENCES

1. Kallos, G.; Kassomenos, P.; Pielke, R.A. Synoptic and Mesoscale Weather Conditions during Air Pollution Episodes in Athens, Greece; *Boundary-Layer Meteorol.* **1993**, *62*, 163-184.
2. Baldasano, J.M.; Calbó, J.; Costa, M. Importance of Atmospheric Transport Processes in the Urban Air Quality: The Case of Barcelona. In *Urban Air Pollution I*; Power, H., Moussiopoulos, N., Brebbia, C.A., Eds.; Computational Mechanics Publications: Southampton, UK, 1995; pp 41-68.
3. Lu, R.; Turco, R.P. Air Pollution Transport in a Coastal Environment II: Three-Dimensional Simulations over Los Angeles Basin; *Atmos. Environ.* **1995**, *29* (13), 1499-1518.
4. Moussiopoulos, N.; Sahm, P.; Kessler, C.; Kunz, R. Numerical Simulation of Photochemical Smog Formation in Athens—A Case Study; *Atmos. Environ.* **1995**, *29* (24), 3619-3632.
5. Millán, M.M.; Salvador, R.; Mantilla, E.; Artíñano, B. Meteorology and Photochemical Air Pollution in Southern Europe: Experimental Results from EC Research Projects; *Atmos. Environ.* **1996**, *30*, 1909-1924.
6. Soriano, C.; Rocadenbosch, F.; Puente, C.; Rodríguez, A.; Baldasano, J.M.; Comerón, A. Confirmation of a Multilayer Arrangement of Aerosols in the Barcelona Air Basin Using Two Independent Lidar Systems. In *Spectroscopic Atmospheric Environmental Monitoring Techniques*; SPIE Proceedings Series; Schäfer, K, Ed.; SPIE: Bellingham, WA, 1998; Vol. 3593; pp 212-222.
7. Soriano, C.; Baldasano, J.M.; Buttler, W.T.; Moore, K. Circulatory Patterns of Air Pollutants within the Barcelona Air Basin in a Summertime Situation: Lidar and Numerical Approaches; *Boundary-Layer Meteorol.* **2001**, *98*, 33-55.
8. Barros, N.; Borrego, C. Influence of Coastal Breezes on the Photochemical Production over the Lisbon Region. In *Air Pollution III, Vol. 3: Urban Pollution*; Moussiopoulos, N., Power, H., Brebbia, C.A., Eds.; Computational Mechanics Publications: Southampton, UK, 1985; pp 67-74.
9. Barros, N. Poluição atmosférica por foto-oxidantes: O ozono troposférico na região de Lisboa. Ph.D. Thesis, Universidade de Aveiro, Portugal, 1999; p 227.
10. *Ozone Position Paper*; Ad Hoc Working Group on Ozone Directive and Reduction Strategy Development: European Communities, July 1999; p 171.
11. Nadal, J.M. El Clima de Baleares. Ph.D. Dissertation, University of Barcelona, 1980.
12. Coronas, A.; Baldasano, J.M. Fourier Analysis of Meteorological Data to Obtain a Typical Annual Time Function; *Solar Energy* **1984**, *32* (4), 478-488.
13. *Ambiente atmosférico em zonas costeiras: Avaliação da capacidade de carga dos ecossistemas*; Relatório de execução material; Projecto AMAZOC; Borrego, C. et al., Contrato Praxis nr. 3/3.2/AMB/38/94, 1999; p 213.
14. Ebel, A.; Elbern, H.; Hass, H.; Jakobs, H.J.; Memmesheimer, M.; Bock, H.J. Meteorological Effects on Air Pollution Variability on Regional Scales. In *Air Pollution III*; Moussiopoulos, N., Power, H., Brebbia, C.A., Eds.; Computational Mechanics Publications: Southampton, UK, 1995; Vol. 4; pp 1-6.
15. Hass, H.; Builtjes, P.J.H.; Simpson, D.; Stern, R. Comparison of Model Results Obtained with Several European Regional Air Quality Models; *Atmos. Environ.* **1997**, *31* (19), 3259-3279.
16. Tchepel, O.; Barros, N.; Borrego, C.; Nunes, T. Mapping Anthropogenic and Biogenic Emissions Data in Portugal. In *Proceedings do IV Encontro de Utilizadores de Sistemas de Informação Geográfica e I Congresso de Informação Geográfica*, ESIG/97, Lisbon, Portugal, 1997.
17. Costa, M.; Baldasano, J.M. Development of a Source Emission Model for Atmospheric Pollutants in the Barcelona Area; *Atmos. Environ.* **1996**, *30A* (2), 309-318.
18. Nunes, M. *Desenvolvimento de uma base de dados de emissões para modelos fotoquímicos de qualidade do ar*; Relatório interno da disciplina de projecto; DAOUA: Aviero, Portugal, 1994.
19. Gómez, O.; Baldasano, J.M. Biogenic VOC Emission Inventory for Catalonia, Spain. In *Proceedings of EUROTRAC Symposium '98*; Borrell, P.M., Borrell, P., Eds.; WIT Press: Southampton, UK, 1999; pp 109-115.
20. *User's Guide to the Systems Applications International Mesoscale Model*; SYSAPP-95/070; Systems Applications International: San Rafael, CA, 1995.
21. Borrego, C.; Barros, N.; Miranda, A.I.; Carvalho, A.C.; Valinhas, M.J. Validation of Two Photochemical Numerical Systems under Complex Mesoscale Circulations. In *Proceedings of the 23rd NATO-CCMS International Technical Meeting on Air Pollution Modelling and Its Application*, Varna, Bulgaria, 1998; pp 411-418.
22. Moussiopoulos, N. *The EUMAC Zooming Model. Model Structure and Applications*; EUROTRAC: Garmisch-Partenkirchen, Germany, 1994; pp 1-266.
23. Simpson, D.; Andersson-Sköld, Y.; Jenkin, M.E. *Updating the Chemical Scheme for the EMEP MSC-W Oxidant Model: Current Status*; EMEP MSC-W Note 2/93; Oslo, 1993.
24. Toll, I.; Baldasano, J.M. Photochemical Modeling of the Barcelona Area with Highly Disaggregated Anthropogenic and Biogenic Emissions; *Atmos. Environ.* **2000**, *34* (19), 3069-3084.
25. Wakimoto, R.M.; McElroy, J.L. Lidar Observation of Elevated Pollution Layers over Los Angeles; *J. Climate Appl. Meteorol.* **1986**, *25*, 1583-1599.

**About the Authors**

Nelson Barros is a professor in the Department of Science and Technology at the University of Fernando Pessoa, Porto, Portugal. Isabel Toll and Pedro Jiménez are Ph.D. students in the Environmental Engineering Program at the Laboratory of Environmental Modeling (LMA), Technical University of Catalonia, Barcelona, Spain. Cecilia Soriano is a postdoctoral researcher at LMA. Carlos Borrego is a full professor in the Department of Environment and Planning at the University of Aveiro, Portugal. José Maria Baldasano is a full professor in Environmental Science and Technology in the High Technical School of Industrial Engineers at the Technical University of Catalonia. Correspondence should be addressed to Dr. José Maria Baldasano, Laboratory of Environmental Modeling, Universitat Politècnica de Catalunya, Av. Diagonal 647, pl. 10, 08028 Barcelona, Spain; e-mail: jose.baldesano@upc.es.